

1 **Ammonia Flux Measurements above a Corn Canopy using Relaxed Eddy**  
2 **Accumulation and a Flux Gradient System**

3  
4 Andrew J. Nelson<sup>1,2</sup>, Nebila Lichiheb<sup>3</sup>, Sotiria Koloutsou-Vakakis<sup>1\*</sup>, Mark J. Rood<sup>1</sup>, Mark  
5 Heuer<sup>3,4</sup>, LaToya Myles<sup>3</sup>, Eva Joo<sup>5</sup>, Jesse Miller<sup>5</sup>, and Carl Bernacchi<sup>5,6</sup>

6  
7 <sup>1</sup>*Department of Civil and Environmental Engineering, University of Illinois at*  
8 *Urbana-Champaign, 205 North Mathews Avenue, Urbana, IL 61801-2352, USA*

9  
10 <sup>2</sup>*U.S. Army Corps of Engineers, Engineer Research and Development Center, International*  
11 *Research Office, Ruislip, HA4 7HB, UK*

12  
13 <sup>3</sup>*National Oceanic and Atmospheric Administration, Atmospheric Turbulence and Diffusion*  
14 *Division, Oak Ridge, TN 37831-2456, USA*

15  
16 <sup>4</sup>*Oak Ridge Associated Universities, Oak Ridge, TN 37830, USA*

17  
18 <sup>5</sup>*Department of Plant Biology and the Energy Biosciences Institute, University of Illinois at*  
19 *Urbana-Champaign, 1206 West Gregory Drive, Urbana, Illinois 61801, USA*

20  
21 <sup>6</sup>*USDA-ARS Global Change and Photosynthesis Research Unit, Urbana, IL 61801, USA*

22  
23  
24 *\*Corresponding Author: [sotiriak@illinois.edu](mailto:sotiriak@illinois.edu) (217) 265-7646*

25  
26 **Keywords:** Ammonia, Bi-directional Flux, Corn, Relaxed Eddy Accumulation, Flux  
27 Gradient, Urease Inhibitor

28  
29 **Highlights:**

- 30
- 31 • Inter-comparison of relaxed eddy accumulation and flux gradient measurements
  - 32 • Strong correlation between the two NH<sub>3</sub> flux measurement methods
  - 33 • Peak NH<sub>3</sub> flux measured with both systems six days after fertilizer application
  - 34 • Two elevated emission periods influenced by urease inhibitor and environmental conditions
- 35

# 1 **Abstract**

2       Studies of NH<sub>3</sub> flux over agricultural ecosystems in the USA are limited by low temporal  
3 resolution (typically hours or days) and sparse spatial coverage, with no studies over corn  
4 in the Midwest USA. We report on NH<sub>3</sub> flux measurements over a corn canopy in Central  
5 Illinois, USA, using the relaxed eddy accumulation (REA) and flux gradient (FG) methods,  
6 providing measurements at 4 h and 0.5 h intervals, respectively. The REA and FG systems  
7 were operated for the duration of the 2014 corn-growing season. Flux-footprint analysis  
8 was used to select data from both systems, resulting in 82 concurrent measurements. Mean  
9 NH<sub>3</sub> flux of concurrent measurements was  $205 \pm 300 \text{ ng m}^{-2} \text{ s}^{-1}$  from REA and  $110 \pm 256 \text{ ng}$   
10  $\text{m}^{-2} \text{ s}^{-1}$  from FG for all concurrent samples. Results from both methods were not  
11 significantly different at a 95% confidence level for all concurrent measurements. The FG  
12 system resolved NH<sub>3</sub> emission peaks at 0.5 h averaging time that were otherwise un-  
13 observed with 4 h REA averaging. Two early-season emission periods were identified (DOY  
14 130-132 and 140-143), where the timing and intensity of such emissions were attributed  
15 to a combination of urease inhibitor, applied as a field-management decision, and localized  
16 soil temperature and precipitation. Given the dependence of NH<sub>3</sub> fluxes on multiple  
17 parameters, this study further highlights the need for increased spatial coverage and high  
18 temporal resolution (*e.g.*, < 1 h) of measurements to better understand the impact of  
19 agricultural NH<sub>3</sub> emissions on air quality and the global nitrogen cycle. Such measurements  
20 are also needed for evaluation of models describing surface-atmosphere exchange of NH<sub>3</sub>.

21

# 1 Introduction

## 2 1.1 Reactive Nitrogen and Anthropogenic Ammonia

3 Continued population growth has resulted in increased demand for food, yielding  
4 perturbations to the global nitrogen cycle (Erisman et al., 2013). While the use of nitrogen-  
5 based fertilizers for food production has improved the ability to cultivate crops in nitrogen-  
6 limited ecosystems, emission of  $\text{NH}_3$  from fertilized cropland results in adverse  
7 environmental effects (USEPA, 2011). According to the U.S. EPA 2014 National Emission  
8 Inventory (NEI), 95% of total atmospheric  $\text{NH}_3$  emission is attributed to anthropogenic  
9 sources (USEPA, 2017). Fertilizer application accounts for 28% of anthropogenic  $\text{NH}_3$   
10 emissions in the USA and is regionally varied based on land use (USEPA, 2017). Fertilizer  
11 application accounts for 52% of anthropogenic  $\text{NH}_3$  emission in Illinois (USEPA, 2017).  $\text{NH}_3$   
12 volatilized from cropland to the atmosphere reacts with acidic compounds in the  
13 atmosphere to form particulate matter with diameter  $\leq 2.5 \mu\text{m}$  ( $\text{PM}_{2.5}$ ), causing adverse  
14 health effects and contributing to wet and dry deposition of reactive nitrogen that can lead  
15 to deleterious environmental effects including waterway eutrophication and soil  
16 acidification (Galloway et al., 2008; Green et al., 2012).

17 Urea-ammonium nitrate (UAN) solution is commonly used as a synthetic nitrogen  
18 fertilizer in Illinois (UI, 2009). After application of UAN to bare soil, the urease enzyme,  
19 present in soils, catalyzes the hydrolysis of urea to  $\text{NH}_4^+$  and, depending on weather  
20 conditions and soil properties (*e.g.*, moisture, temperature, and pH), results in part of the  
21 applied reactive nitrogen volatilizing as  $\text{NH}_3$  to the atmosphere (Fenn and Hossner, 1985).  
22 However, the use of N-(n-butyl)-thiophosphoric triamide (nBTPT) urease inhibitor can

1 reduce NH<sub>3</sub> emission by inactivating the site of the enzyme responsible for catalyzing the  
2 hydrolysis reaction (Watson et al., 1994). Chadwick et al. (2005) reported reductions of  
3 NH<sub>3</sub> emission from UAN ranging from 15 – 71% (44% mean reduction, number of samples  
4 = 10) when nBTPT urease inhibitor was used on grasslands and cereal crops.

5 Successful SO<sub>x</sub> and NO<sub>x</sub> regulatory policies combined with increased use of nitrogen-  
6 based fertilizers have led to an increased amount of NH<sub>3</sub> and NH<sub>4</sub><sup>+</sup> in the environment, as  
7 evidenced by a shift of reactive nitrogen deposition in the USA from oxidized to reduced  
8 nitrogen (Li et al., 2016). However, further regulation of NO<sub>x</sub> and SO<sub>x</sub> may no longer be cost  
9 beneficial when compared with control of NH<sub>3</sub> emissions to reduce atmospheric particulate  
10 matter concentration (Pinder et al., 2007). Improved understanding of NH<sub>3</sub> fluxes is  
11 important to more fully characterize their impact on the global nitrogen cycle, develop  
12 targeted strategies for emission reductions, and reduce the formation of secondary air  
13 pollutants (Flechard et al., 2013; Li et al., 2016).

## 14 *1.2 Quantification of Ammonia Flux*

15 The U.S. EPA Science Advisory Board (SAB) has called for increased direct  
16 measurements of NH<sub>3</sub> emission from agricultural cropland to better understand nitrogen  
17 fertilizer use efficiency (NFUE) and to identify regions and crop types that contribute  
18 significantly to anthropogenic NH<sub>3</sub> emissions to the atmosphere (USEPA, 2011). Limited  
19 measurements of NH<sub>3</sub> emissions contribute to poor temporal and spatial representation of  
20 NH<sub>3</sub> in regional air quality models (Appel et al., 2011) and restrict the ability to evaluate  
21 models developed to predict NH<sub>3</sub> emissions (Balasubramanian et al., 2017). Existing  
22 models (Bash et al., 2010) and measurements using accumulation methods (Walker et al.,

1 2013; Nelson et al., 2017) suggest that NH<sub>3</sub> emissions are not temporally uniform and are  
2 influenced by local environmental conditions that can change on the order of minutes.

3 Measurement of biosphere-atmosphere NH<sub>3</sub> flux is challenging because NH<sub>3</sub> is readily  
4 absorbed by water and is reactive with acidic species in the atmosphere (Sutton et al.,  
5 2007), while gaseous NH<sub>3</sub> co-exists with particulate NH<sub>4</sub><sup>+</sup>. Low concentrations of NH<sub>3</sub>  
6 previously observed at agricultural sites (*i.e.*, 0.5 – 4 μg m<sup>-3</sup> two weeks after fertilizer  
7 application) (Nelson et al., 2017) limit the suitability of several fast response (10 Hz)  
8 detectors due to higher detection limits (0.10 μg m<sup>-3</sup> NH<sub>3</sub> at 10 Hz with total accuracy of  
9 0.14 μg m<sup>-3</sup> NH<sub>3</sub> ± 10 %; Miller et al., 2014). Many reported measurements of NH<sub>3</sub> flux from  
10 agricultural crop systems rely on chemical adsorption and/or accumulating methods to  
11 quantify flux, resulting in temporal resolutions of hours or days (Myles et al., 2007; Walker  
12 et al., 2013; Nelson et al., 2017).

13 Recent improvements to instrument detection limits have resulted in several  
14 demonstrations of fast-response closed eddy covariance (EC) systems for measuring NH<sub>3</sub>  
15 flux from cattle feedlots (Ferrara et al., 2014; Sintermann et al., 2011). However, such  
16 systems are limited by reactivity of NH<sub>3</sub> in sample lines and inlets that can affect high-  
17 frequency response and result in underestimation of NH<sub>3</sub> flux (Ferrara et al., 2014). Open-  
18 path EC systems are a promising alternative to improve fast-response measurement as  
19 they avoid the potential interference from sampling lines. Such a system was used for  
20 measurement of NH<sub>3</sub> flux at cattle feedlots, with a limit of detection for NH<sub>3</sub> flux of 1.3 ± 0.5  
21 ng m<sup>-2</sup> s<sup>-1</sup> over a 30-min average (Sun et al., 2015). However, the exposed optics make long-

1 duration measurement (*i.e.*, > 1 day) in an open agricultural field challenging due to fouling  
2 of the optical cell by airborne dust and insects (Miller et al. 2014).

3 Improved temporal resolution of measurements during the early-season period are  
4 needed to better understand the variability of NH<sub>3</sub> flux (Walker et al. 2013) and to quantify  
5 the benefit of urease inhibitors on reducing NH<sub>3</sub> volatilization at the field scale (Nelson et  
6 al., 2017). Further, existing process-based models to describe surface-atmosphere  
7 exchange of NH<sub>3</sub> at sub-hourly timescale, such as SURFATM-NH<sub>3</sub> (Personne et al., 2009)  
8 which simulates the bi-directional exchange of NH<sub>3</sub> with vegetation and Volt'air-NH<sub>3</sub> which  
9 simulates NH<sub>3</sub> fluxes from bare soil (Génermont and Cellier, 1997; Garcia et al., 2012)  
10 require field-scale measurements at similar timescales for evaluation. Walker et al. (2013)  
11 suggested that existing NH<sub>3</sub> models may be least suited to accurately predict emissions  
12 during the first month after fertilizer application, when emissions are highest and most  
13 variable.

### 14 *1.3 Research Motivation and Significance*

15 In this paper, we present an inter-comparison of NH<sub>3</sub> flux measurements above a corn  
16 canopy in Central Illinois, USA, using relaxed eddy accumulation (REA) and the flux  
17 gradient (FG) measurement methods. This inter-comparison provides an important  
18 understanding of the efficacy of the FG method when compared with the REA method,  
19 which has been more extensively used for NH<sub>3</sub> flux measurement in varied ecosystems  
20 (Zhu et al., 2000; Meyers et al., 2006; Myles et al., 2007) and in Central Illinois, USA (Nelson  
21 et al., 2017). FG can yield sub-hourly temporal resolution of NH<sub>3</sub> flux and has been used to  
22 measure NH<sub>3</sub> fluxes over a variety of managed agricultural ecosystems including grassland

1 (Sutton et al., 2001; Spindler et al., 2001; Milford et al., 2009), corn (Harper and Sharpe,  
2 1995), triticale (Loubet et al., 2012) wheat (Personne et al., 2015), and unfertilized soybean  
3 (Myles et al., 2011). However, measurements at sub-hourly timescale have not been  
4 reported for corn managed under typical agricultural practices and under the  
5 micrometeorological conditions in the Midwest USA.

6 Enhanced temporal resolution of NH<sub>3</sub> flux measurements provided by FG is important  
7 to improve the understanding of the impact of localized environmental parameters on NH<sub>3</sub>  
8 flux intensity and to evaluate local and regional modeling of NH<sub>3</sub> flux (Flechard et al., 2013;  
9 Walker et al., 2013). Further, FG provides a beneficial method for characterizing diurnal  
10 patterns of NH<sub>3</sub> flux, which has not previously been reported in the literature for typical  
11 field-management practices in Illinois. This research inter-compares concurrent REA  
12 measurements of NH<sub>3</sub> flux over an intensively managed corn field in Central Illinois, USA  
13 (Nelson et al., 2017) with new 30 min averaged NH<sub>3</sub> flux measurements from a  
14 continuously operated FG system. These new measurements, and the inter-comparison of  
15 experimental methods, are important to improve our understanding of temporal variability  
16 of NH<sub>3</sub> fluxes. They are also important for micrometeorological measurement method  
17 evaluation and further development of such methods in diverse environments in terms of  
18 climate, topography, and land use. These results can be used to further enhance NH<sub>3</sub>  
19 emission model evaluations and to improve understanding of the impact of intensively  
20 managed agricultural ecosystems on air quality and the global nitrogen cycle.

## 1 **2. Methods**

### 2 *2.1 Site Description and Field Management Practices*

3 The field campaign was conducted during the 2014 corn-growing season at the  
4 University of Illinois at Urbana-Champaign (UIUC) Energy Biosciences Institute (EBI)  
5 Energy Farm in Illinois, USA. A complete description of field management practices and  
6 geographic features of the Energy Farm and surrounding area, and methods for measuring  
7 crop height and leaf area index (LAI) is presented in Nelson et al. (2017). Briefly, the  
8 Energy Farm was subdivided into four 200 m x 200 m research plots, each planted with  
9 one of either miscanthus, switchgrass, restored prairie, or corn. This research was  
10 conducted at the corn plot (hereafter referred to as the “study plot”) during the first year of  
11 a corn-corn-soybean rotation. No artificial irrigation was applied to the study plot.

12 The study plot was treated with 168 kg-N ha<sup>-1</sup> as 28% urea-ammonium nitrate (UAN)  
13 fertilizer in water (Illini FS: Urbana, IL), 7.0 L ha<sup>-1</sup> pre-emergent herbicide (Lumax®,  
14 Syngenta: Basel, Switzerland), and 3.36 kg ha<sup>-1</sup> urease inhibitor (Agrotain® DRI-MAXX  
15 [0.0625 % w/w of UAN], Koch Agronomic Services: Wichita, KS, USA), on May 6, 2014 (DOY  
16 126). The study plot was tilled and machine-sown with corn (Dekalb®, DKC64-69,  
17 Monsanto: St. Louis, MO) at 76 cm row spacing to a seeded population of 86,000 plants ha<sup>-1</sup>  
18 in the afternoon on DOY 126. Herbicide (Roundup® Powermax, Monsanto: St. Louis, MO)  
19 was applied at 1.6 L ha<sup>-1</sup> on June 6, 2014 (DOY 157) and additionally spot applied as  
20 needed.



1            *2.2 NH<sub>3</sub> Flux Measurements*

2            The REA system was setup and operational in the afternoon on DOY 126, 4 h after corn  
3 planting at the study plot. The FG system was setup over the following two days, and was  
4 operational on DOY 129. The study plot was serviced with two 20 A electrical circuits, both  
5 of which were required to operate the computers and pumps associated with the  
6 measurement systems. The REA and FG systems were 5 m apart at the center of the study  
7 plot, fully surrounded by corn (Figure 1).



8  
9            **Figure 1:** The relaxed eddy accumulation (left tower) and flux gradient (right tower) measurement systems  
10 were located 5 m apart in the center of the study plot.

11            *2.2.1 Relaxed Eddy Accumulation System*

12            The REA system used for this field campaign is described by Nelson et al. (2017), but a  
13 brief description is provided here for improved clarity. Additionally, an evaluation of  
14 closure between REA measurements reported in Nelson et al. (2017) and modeled outputs  
15 using the DeNitrification DeComposition (DNDC) model is presented in Balasubramanian

1 et al. (2017), where agreement between modeled and measured results was found to be  
2 best during the first 30 days after fertilizer application.

3 The mean vertical flux from REA,  $\overline{F_{REA}}$  ( $\text{ng m}^{-2} \text{s}^{-1}$ ), is estimated using Equation 1:

$$4 \quad \overline{F_{REA}} = \beta \sigma_w (\overline{C^\uparrow} - \overline{C^\downarrow}) \quad 5 \quad (1)$$

6 where  $\beta$  is the REA coefficient (unitless),  $\sigma_w$  is the standard deviation of the vertical wind  
7 velocity,  $C$  is concentration ( $\text{ng m}^{-3}$ ), overbars denote time averaging, and  $\uparrow$  and  $\downarrow$  denote  
8 up- and down-draft measurements, respectively. The REA coefficient is estimated from 10  
9 Hz measurements of temperature from a sonic anemometer using Equation 2:

$$10 \quad \beta = \frac{\overline{w'T'}}{\sigma_w (\overline{T^\uparrow} - \overline{T^\downarrow})} \quad 12 \quad 13 \quad (2)$$

14 1 where  $w$  is vertical wind speed ( $\text{m s}^{-1}$ ),  $T$  is temperature (K), and primes ( $'$ ) denote  
15 instantaneous deviations from the mean. The Eddy Accumulation (EA) method, originally  
16 introduced by Desjardins (1972), required that sample flow rates in up- and down-draft  
17 reservoirs be controlled proportionally with vertical wind speed. Businger and Oncley  
18 (1989) “relaxed” the EA method requirement by introducing the REA coefficient. The REA  
19 coefficient is a proportionality constant that accounts for the impact of vertical wind speed  
20 while sampling at a constant flow rate, thereby eliminating the complication associated  
21 with proportional sampling flow rates.

22 The REA system was operated intermittently throughout the growing season, with  
23 more sampling concentrated during the first 30 days following fertilizer application. No  
24 REA measurements were made during precipitation events to avoid aspiration of water  
25 into the denuders. REA samples were collected from 07:30 – 11:30 and 12:00 – 16:00 (all

1 times are reported as local) to represent average meteorological conditions and avoid  
2 sampling during atmospheric stability transitions at dawn and dusk. The REA system was  
3 not used to collect nighttime samples as it is not expected to perform well during highly  
4 stable atmospheric conditions (Fotiadi et al., 2005).

5 Gas flow and switching of denuders during updraft, downdraft, and deadband  
6 conditions was controlled via a system similar to the one described by Meyers et al. (2006)  
7 with a field computer running the open source program SONIC.C (version 2.6.0, NOAA  
8 ATDD, SONIC program for Linux, Oak Ridge, TN). Flow rate through the denuders was fixed  
9 at 20.0 L min<sup>-1</sup> using a mass flow controller (MFC) (model GFC371, Aalborg: Orangeburg,  
10 NY). The control system was connected to a three-axis ultrasonic anemometer (model  
11 81000VRE, R.M. Young Company: Traverse City, MI) measuring wind speed in three  
12 directions ( $u$ ,  $v$ , and  $w$ ) and sonic temperature ( $T$ ), at 10 Hz.

13 Phosphorous acid coated annular denuders (model URG-2000-30x242-3CSS, URG Corp:  
14 Chapel Hill, NC) were used to collect NH<sub>3</sub> in the REA system. All denuders were coated,  
15 extracted, and analyzed at the National Atmospheric Deposition Program (NADP) Central  
16 Analytical Laboratory (CAL). CAL used quality assurance procedures to mitigate potential  
17 contamination of samples (NADP, 2012). At least one laboratory blank and one field blank  
18 were used for every 20 denuders prepared. Four denuders were used for each REA  
19 sampling run: one each for updraft, deadband, and downdraft conditions and one as a field  
20 blank. Each REA sampling run lasted at least 4 h, guided by the analytical detection limit for  
21 NH<sub>4</sub><sup>+</sup> and typical ambient NH<sub>3</sub> concentrations in the area (Nelson et al., 2017).

### 2.2.2 Flux Gradient System

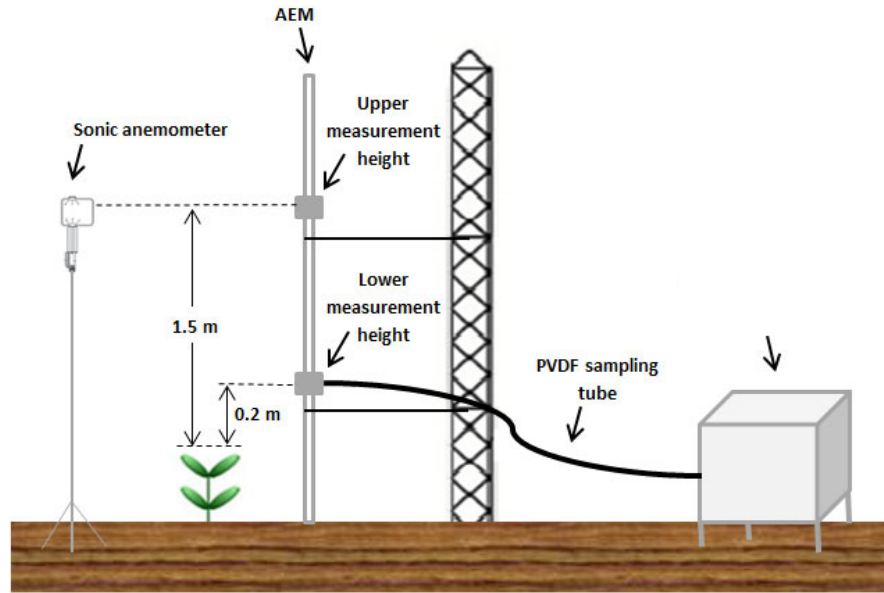
The FG technique is theoretically described by analogy to Fick's laws of diffusion, with an assumption that turbulent transfer is analogous to molecular diffusion. The turbulent flux is therefore proportional to the product of the mean vertical mixing ratio gradient and the vertical eddy diffusivity,  $K$  (Baldocchi et al., 1988). By assuming mass and energy are transported by the same eddies, eddy diffusivities are assumed equal among scalars and heat in the atmosphere. Hence, the FG technique assumes that the eddy diffusivity of each tracer gas is identical to the measured eddy diffusivity of heat (Hicks and Wesely, 1978). Based on this assumption,  $K$  is determined directly by combining the measured eddy covariance flux of temperature ( $F_H$ ) and gradient measurements of temperature and concentration. Thus, the  $\text{NH}_3$  flux from FG ( $F_{FG}$ ) is calculated using Equation 3:

$$F_{FG} = -K_H \left( \frac{\Delta C_{\text{NH}_3}}{\Delta Z} \right) = F_H \left( \frac{\Delta C_{\text{NH}_3}}{\Delta T} \right) \quad (3)$$

where  $K_H$  is the eddy diffusivity for sensible heat ( $\text{m}^2 \text{s}^{-1}$ ),  $\Delta C_{\text{NH}_3}$  is the difference in  $\text{NH}_3$  concentration ( $\text{ng m}^{-3}$ ) between two measurement heights,  $\Delta Z$  is the vertical distance between the two measurement points (m) and  $\Delta T$  is the corresponding difference in temperature (K). Eddy covariance measurements of temperature flux were used to determine  $K_H$  (Myles et al., 2011).

The FG system is graphically depicted in Figure 2. The vertical distance between the two measurement heights was kept constant ( $\Delta z = 1.3 \text{ m}$ ) with a lowest initial measurement height of  $z = 0.4 \text{ m}$  above the ground prior to corn emergence. Sampling height was adjusted with an automated exchange mechanism (AEM) (REBS Inc.: Bellevue,

1 WA). The AEM design was similar in principle to that described by Gay and Fritschen  
2 (1979). After emergence, measurement height was adjusted weekly such that  $z = 0.2$  m and  
3 1.5 m above the canopy.



4  
5 **Figure 2:** Schematic of the flux gradient (FG) sampling system with an automated exchange mechanism  
6 (AEM), cavity ring down spectrometer (CRDS), and polyvinylidene fluoride (PVDF) sampling tube.

7 In order to determine  $K_H$ , the sensible heat flux was measured by eddy covariance using  
8 a sonic anemometer (model 81000 VRE, R.M. Young: Traverse City, MI) placed at 1.5 m  
9 above the canopy. Temperature and three-dimensional wind speed ( $u, v, w$ ;  $\text{m s}^{-1}$ ) were  
10 measured with the sonic anemometer at 10 Hz using a custom Linux-based acquisition  
11 program developed by the NOAA Atmospheric Turbulence and Diffusion Division (Oak  
12 Ridge, TN) (Meyers et al., 1996). Measurements of temperature at the lower and upper  
13 measurement heights were made with resistance thermometers ( $1000 \Omega$  Platinum  
14 Thermometer, Thermometrics Corp.: Northridge, CA) housed in aspirated radiation shields

1 (model 43502, R.M. Young: Traverse City, MI) to minimize solar heating effects. 30-min  
2 average values of  $K_H$  were calculated using Equation 4:

$$3 \quad K_H = - \frac{\overline{w'T'}}{(\Delta T / \Delta z)} \quad (4)$$

4 Concentration of  $\text{NH}_3$  was measured using a cavity ring-down spectroscopy (CRDS)  
5 instrument (model G2103, Picarro Inc.: Santa Clara, CA) starting at the lower height for 7  
6 min then switching to the upper height for 8 min and reversing the timing (i.e., 8 then 7 min  
7 at lower and upper heights, respectively). The lower detection limit of this instrument for  
8  $\text{NH}_3$  is  $< 0.06 \mu\text{g m}^{-3}$  with an accuracy of ( $\pm 5 \%$  of reading +  $0.35 \mu\text{g m}^{-3}$ ) at a 300 s  
9 averaging time. CRDS is a laser absorption technique, which measures the lifetime of  
10 photons reflected between two mirrors in an optical cavity and determines the sum of  
11 sample extinction between the cavity mirrors, enabling quantification of  $\text{NH}_3$  concentration  
12 by the strength of near-infrared absorption. (Scherer et al., 1997). The advantage of this  
13 method is that it allows absorption measurements using very long optical path lengths  
14 (effective path length up to 20 km) while maintaining a closed optical cell to enable single  
15 point measurements and limit contamination (Moosmüller et al., 2005).

16 The CRDS system was connected to a rotary pump (model 0523, Gast Manufacturing  
17 Inc.: Benton Harbor, MI) sampling at  $70 \text{ L min}^{-1}$ . The CRDS and pump were housed in an  
18 air-conditioned enclosure unit in which the temperature was adjusted to  $10 \text{ }^\circ\text{C}$  below  
19 ambient to prevent overheating. The CRDS was calibrated by the manufacturer.

20 Additionally, the calibration was verified using a short polyvinylidene fluoride (PVDF)  
21 vented inlet tube, and zero and span compressed gas cylinders according to manufacturer  
22 directions. The zero check was performed with ultrahigh purity nitrogen (99.999%) and

1 the span adjustment was performed using  $715.8 \mu\text{g m}^{-3}$  ( $1030 \text{ ppb} \pm 5 \%$ )  $\text{NH}_3$  (NIST-  
2 traceable reference gas; Air Liquide: Plumsteadville, PA). The zero and span checks were  
3 within the tolerance of the manufacturer's calibration with offset of  $\sim 0.8 \text{ ppb}$  and span of  
4  $\sim 1135 \text{ ppb}$ .

5 An inlet tube was used to transfer air to the CRDS because it was housed in an enclosure  
6 and was situated in an agricultural field. Due to the high water solubility and polarity of  
7  $\text{NH}_3$ , the choice of the sampling tube material was carefully investigated. PVDF was selected  
8 for use as the tubing material based on an experimental study by Vaittinen et al. (2014)  
9 that found it to be the least adsorbent polymer of five tested. An 8 m PVDF sampling tube  
10 (25.4 mm OD, 22.2 mm ID, McMaster-Carr: Elmhurst, IL) was used for the inlet line. The  
11 sampling tube was warmed with heating tape to  $5 \text{ }^\circ\text{C}$  above ambient temperature to  
12 prevent condensation and limit  $\text{NH}_3$  loss. The sampling tube was attached to the AEM  
13 allowing vertical movement.

14  $\text{NH}_3$  fluxes were continuously monitored (24 h/day) during the first three months of  
15 the 2014 corn-growing season (DOY 129 – 212), starting two days after fertilizer  
16 application and planting.  $\text{NH}_3$  concentrations were averaged over 30 min. Due to  
17 precipitation events that blocked the sonic anemometer, 1.5% of overall samples were not  
18 collected. Furthermore, data corrections were conducted to limit interference from water  
19 vapor (Martin et al., 2016) and due to increasing pressure drop across the CRDS internal  
20 filter over time due to aspirated particulate dust, which contributes to increased response  
21 time. The response time of the  $\text{NH}_3$  system was measured at the beginning and end of the  
22 corn-growing season, then corrected using the method of McCarthy (1973), based on a

1 least squares exponential curve fit. The response time for the correction ranged from 4.8  
2 min to 10.5 min. NH<sub>3</sub> data were smoothed to remove noise using a cubic spline filter. Data  
3 were further processed by removing measurements where the magnitude of the measured  
4 NH<sub>3</sub> flux exceeded the population mean by more than five standard deviations (SD). The  
5 use of five SD was compared with three SD as a cutoff prior to processing. Five SD was  
6 selected because of the relatively small difference in total data removed when compared  
7 with three (i.e., of 1458 data points remaining after footprint correction, 1447 data points  
8 remained after applying five SD and 1409 data points after applying three SD). This was  
9 further guided by a goal to limit exclusion of data associated with short-term (< 1 h)  
10 emission peaks.

11 NH<sub>3</sub> flux was calculated in 30 min averages (FG<sub>30min</sub>) using the FG system. In order to  
12 account for possible NH<sub>3</sub> stickiness and response time, after filtering and correcting for the  
13 time constant, the final 3 min of each subsampling period were used for analysis (i.e., 6 min  
14 at each height per half hour period). Subsequently, 240 min average fluxes (FG<sub>240min</sub>) were  
15 calculated from these data to compare with the timescale of REA measurements. FG<sub>240min</sub>  
16 was calculated as a moving boxcar average, where averages were only calculated if FG<sub>30min</sub>  
17 samples existed for the duration of the 240 min period.

### 18 *2.3 Flux Footprint Analysis*

19 Flux footprint was calculated for all REA and FG sampling periods using the EddyPro  
20 software package (Version 5.1.1, LI-COR: Lincoln, NE) (Nelson et al., 2017). The footprint  
21 parameterization described by Kljun et al. (2004) was used as the default option for  
22 footprint estimation. This method is only valid within a certain range of



1 micrometeorological parameters. When measurements were outside this range, the  
2 crosswind integrated model by Kormann and Meixner (2001) was used.

3 Footprint was calculated for NN% = 10%, 30%, 50%, 70%, and 90% distances, where  
4 NN% distance corresponds to the calculated radius (r) of the area that contributed NN% of  
5 the total measured flux. The flux footprint calculation was used to select REA and FG  
6 samples where significant measured NH<sub>3</sub> flux originated from within the study plot (i.e.,  
7 70% and 90%). Samples were selected by comparing the 70% and 90% footprint distances  
8 corresponding to the shortest boundary of the study plot, r = 100 m. For example, if r<sub>70%</sub> <  
9 100 m for a particular sample, it was selected for further analysis.

#### 10 2.4 Inter-comparison of REA and FG Measurements

11 All REA and FG measurements were compared to determine the total number of  
12 concurrent measurements after qualification using both the 70% and 90% footprint  
13 distance. For any 4 h REA measurement, an FG measurement was considered to be  
14 concurrent if there were at least 3 h overlapping data. This data qualification procedure  
15 based on footprint analysis ensures that reported data are representative of fluxes from the  
16 study plot and mitigates the influence of NH<sub>3</sub> emissions from neighboring fields.

17 Data were analyzed to investigate correlation and closure between concurrent  $F_{REA}$   
18 and  $F_{FG240min}$  data. The Pearson correlation coefficient ( $Correl(REA, FG)$ ) was calculated  
19 for all concurrent measurements using Equation 5:

$$20 \quad Correl(REA, FG) = \frac{\sum(F_{FG240min} - \overline{F_{FG240min}})(F_{REA} - \overline{F_{REA}})}{\sqrt{\sum(F_{FG240min} - \overline{F_{FG240min}})^2 \sum(F_{REA} - \overline{F_{REA}})^2}} \quad 21 \quad (5)$$

1 A nonparametric Wilcoxon ranks sum test was also used to evaluate whether there was  
2 statistically significant difference among the two measurement methods at a 0.95  
3 confidence level (Walker et al., 2013).

### 4 **3. Results**

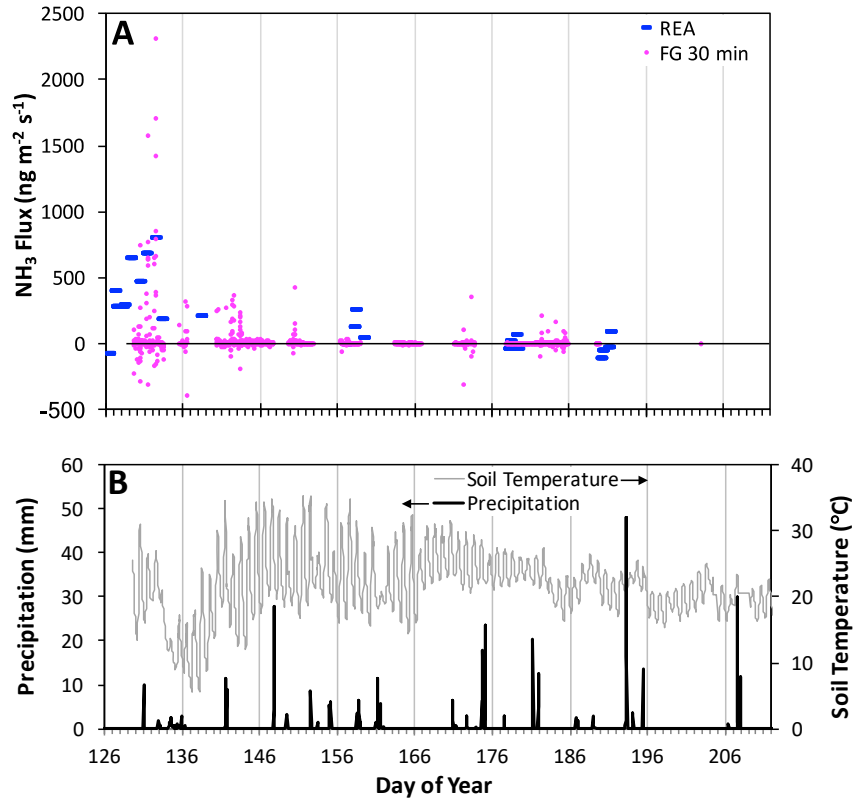
#### 5 *3.1 Canopy Development*

6 Plants were first visible on May 12 (DOY 132), with peak canopy height of 308 cm ± 10  
7 cm measured on July 25 (DOY 206). The canopy reached peak LAI (6.1) on August 13 (DOY  
8 225). Harvesting of the corn was completed on November 6 (DOY 310) with an average  
9 yield of 13.78 mt ha<sup>-1</sup> (219.5 bu acre<sup>-1</sup>), consistent with the average yield in Champaign  
10 County for 2014 of 13.59 mt ha<sup>-1</sup> (216.5 bu acre<sup>-1</sup>) (USDA, 2015).

#### 11 *3.2 Full-Season Flux Measurements*

12 Data presented in this paper are available in the Illinois data bank (Nelson et al., 2018).  
13 Full-season NH<sub>3</sub> flux measurements from the REA and FG systems are presented in Figure  
14 3A (. FG measurements in Figure 3A, reported as 30 min averages (FG<sub>30min</sub>), are selected  
15 based on footprint according to the method described in Section 2.3.

16



1

2

3 **Figure 3:** (A) NH<sub>3</sub> flux as measured using relaxed eddy accumulation (REA, 4 h integrated measurements)  
 4 and 30 min averaged flux gradient (FG<sub>30min</sub>) systems at the study plot for the full growing season (fertilizer  
 5 application occurred on DOY 126). (B) Soil temperature (30 min average) and precipitation (30 min  
 6 accumulated per event).

7 Mean soil temperature was  $21.4 \pm 4.4$  °C, with lowest temperatures observed shortly

8 following fertilizer application (DOY 133 – 140), when mean soil temperature was  $13.5 \pm$

9  $4.6$  °C (Figure 3B). Total precipitation for all data reported in Figure 3B was 1082 mm as

10 rain. Time series and descriptive statistics of additional select monitored variables are

11 shown in Figures S1-S6 in supplementary material (SM), for the same period shown in

12 Figure 3. No correlations were identified between NH<sub>3</sub> fluxes and the variables in SM.

13 Turbulent mixing influences the accuracy of the measurements when micrometeorological

14 methods are used and possibly affect the direction of fluxes. However, the extent to which

15 these variables influence the observed variation of NH<sub>3</sub> fluxes is not easy to establish

1 without a longer time series of continuous flux measurements, including measurements in-  
 2 and above-canopy.

3 A summary of mean, maximum, and minimum NH<sub>3</sub> flux measured using REA and FG is  
 4 presented in Table 1. FG results presented in Table 1 are divided into FG<sub>30min</sub> and FG<sub>240min</sub>  
 5 data. Further, daytime and nighttime mean fluxes are provided for the FG method. REA  
 6 results are not divided into daytime and nighttime measurements because REA was not  
 7 used for nighttime measurements.

	<b>NH<sub>3</sub> Flux (ng m<sup>-2</sup> s<sup>-1</sup>)</b>		
	<b>REA</b>	<b>FG<sub>30min</sub></b>	<b>FG<sub>240min</sub></b>
<b><i>All data</i></b>			
Mean	147 ± 284	23.9 ± 148	12.4 ± 73.2
Maximum	800	2312	1023
Minimum	-161	-400	-93
Daytime	--	25.9 ± 93.5	17.0 ± 85.4
Nighttime	--	-0.23 ± 0.23	0.1 ± 0.1
<b><i>DOY 126 - 156</i></b>			
Mean	431 ± 204	29.4 ± 169	24.0 ± 103
Daytime	--	53 ± 159	34.4 ± 122
Nighttime	--	-0.5 ± 9.0	0.4 ± 6.0
<b><i>After DOY 156</i></b>			
Mean	13.7 ± 99.2	0.8 ± 23.3	1.1 ± 7.1
Daytime	--	1.4 ± 21.1	1.6 ± 7.7
Nighttime	--	0.0 ± 2.0	-0.2 ± 1.8
<b><i>Concurrent data</i></b>			
Mean	205 ± 300	--	110 ± 256

8 **Table 1:** Summary of all NH<sub>3</sub> flux measurements using relaxed eddy accumulation (REA) and flux gradient  
 9 (FG) methods. FG<sub>30min</sub> data correspond to 30 min average fluxes using FG, and FG<sub>240min</sub> are 240 min averages.  
 10 Data are further subdivided based on the first 30 days after planting (DOY 126-156) and the remainder of the  
 11 season (after DOY 156), where DOY is “day of year”.

12 Mean NH<sub>3</sub> fluxes over the entire growing season were 147 ± 284 ng m<sup>-2</sup> s<sup>-1</sup> and 23.9 ±  
 13 148 ng m<sup>-2</sup> s<sup>-1</sup> with REA and FG<sub>30min</sub> data, respectively. The difference in mean flux  
 14 measured with each system is attributed to the higher temporal resolution of the FG

1 system, resulting in FG measurements across more environmental and atmospheric  
2 conditions, including measurements of deposition during nighttime and more  
3 measurements during daytime. Cumulative estimated N percent loss for the whole season was  
4 5.8% and 6.0% from FG and the REA methods, respectively. Cumulative estimated N percent loss  
5 over the first 21 days after fertilizer application were 2.1% and 2.5% for FG and REA, respectively.  
6 Cumulative fluxes were estimated from mean daily fluxes measured with the FG and REA methods.  
7 The REA cumulative N loss percentage is lower than it has been reported before (Nelson et al.,  
8 2017) because the calculation method here was adjusted to account for negligible night time NH<sub>3</sub>  
9 fluxes, based on evidence from the FG continuous measurements, for the specific location.

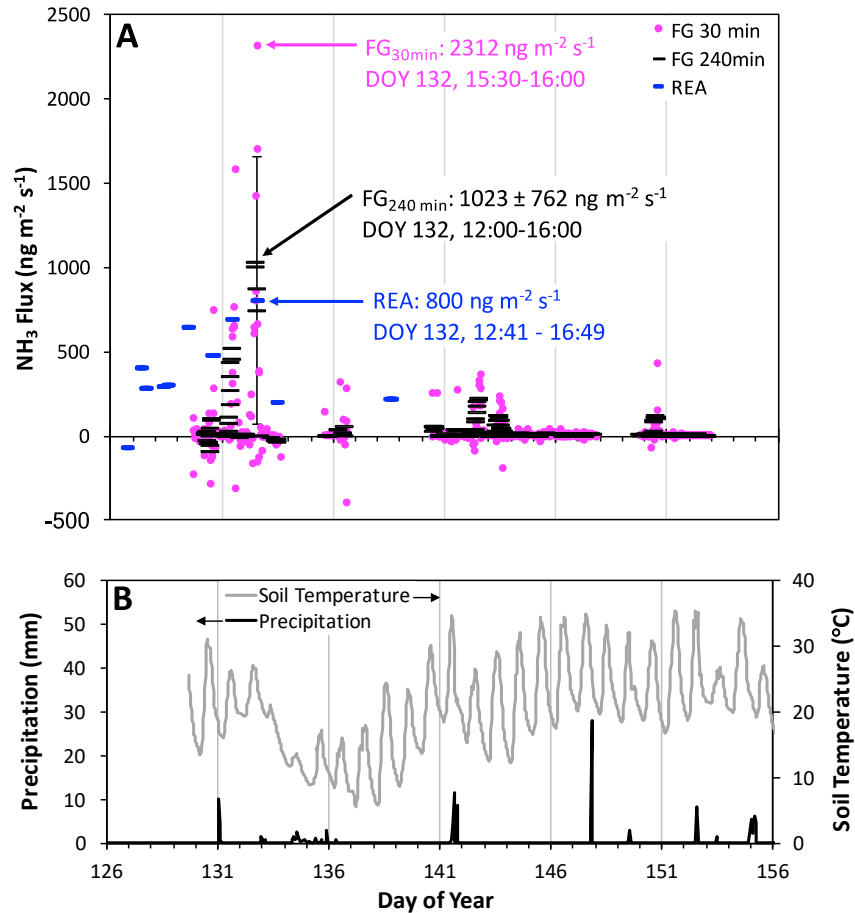
10

### 11 *3.2.1 Early Season Emission and Impact of Timescales*

12 A similar emission trend was observed using both measurement methods. That is, peak  
13 NH<sub>3</sub> emission occurred during the first 30 days after fertilizer application followed by  
14 lower emissions for the remainder of the corn-growing season.

15 Figure 4 presents measurements using REA and FG<sub>30min</sub> for the first 30 days following  
16 fertilizer application as well as precipitation and soil temperature data for the same time  
17 period.

18



1

2  
3  
4  
5  
6  
7  
8

**Figure 4:** (A) Relaxed Eddy Accumulation (REA), 30-min Flux Gradient (FG<sub>30min</sub>), and 240 min Flux Gradient (FG<sub>240min</sub>) measurements of NH<sub>3</sub> flux during the first 30 days after fertilizer application. Error bars represent  $\pm 1$  standard deviation of the mean for the maximum FG<sub>240min</sub> measurement only. (B) Soil temperature and precipitation during the same period.

9 Maximum observed NH<sub>3</sub> emission was 800 ng m<sup>-2</sup> s<sup>-1</sup> with REA and 2312 ng m<sup>-2</sup> s<sup>-1</sup> with  
 10 FG<sub>30min</sub>. The REA emission peak was observed during the 12:41 – 16:49 averaging interval  
 11 on DOY 132 while the FG<sub>30min</sub> peak was observed on the same day during the averaging  
 12 period at 15:30 – 16:00. While the averaging periods for both maxima overlap, results from  
 13 the FG<sub>30min</sub> measurements indicate a high amount of variability. FG<sub>30min</sub> measurements  
 14 ranged from -157 to 2312 ng m<sup>-2</sup> s<sup>-1</sup> between 13:00 and 17:00 on DOY 132 with standard  
 15 deviation of 762. Though the net flux during this time period was positive, there was one

1 FG<sub>30min</sub> sample where deposition was observed (15:00 – 15:30). 10 mm precipitation as  
2 rain occurred on DOY 131, followed by a cold front, resulting in reduced soil temperature  
3 from a maximum of 30.9 °C in the afternoon on DOY 130 (

4 Figure 4B) to a maximum of 13.2 °C in the afternoon on DOY 134. Soil temperature did  
5 not return to 30.9 °C until DOY 141 in the morning.

6 To further investigate the effect of averaging time on the observed variability of NH<sub>3</sub>  
7 flux, REA measurements were compared with FG measurements averaged to 240 min  
8 intervals (FG<sub>240min</sub>). Maximum emission was again observed in the afternoon on DOY 132  
9 for both systems, where max REA flux was 800 ng m<sup>-2</sup> s<sup>-1</sup> from 12:41 to 16:49 and FG<sub>240min</sub>  
10 maximum was 1023 ± 762 ng m<sup>-2</sup> s<sup>-1</sup> from 12:00 – 16:00. The REA and FG<sub>240min</sub> flux maxima  
11 are not statistically different at 95% confidence level, due to the high standard deviation of  
12 the FG<sub>240min</sub> measurement. The FG<sub>240min</sub> peak was shifted earlier in the day by 0.75 h when  
13 compared to REA because emissions were generally higher earlier in the afternoon. As  
14 noted in section 2.2.2, FG<sub>240min</sub> data used for this method comparison represent a subset of  
15 all FG<sub>30min</sub> measurements because they only represent periods when eight consecutive  
16 FG<sub>30min</sub> measurements were available during concurrent REA measurement periods.

17 The maximum 240 min averaged fluxes measured in this study are consistent with  
18 values of midday flux of 700 ± 1100 ng m<sup>-2</sup> s<sup>-1</sup>, reported by Walker et al. (2013). However,  
19 the FG system is capable of resolving the early season emission trend in higher resolution  
20 than previously reported in the literature using accumulating NH<sub>3</sub> flux measurement  
21 techniques (Nelson et al., 2017; Walker et al., 2013). This increased temporal resolution  
22 provides new information about non-stationarity in the NH<sub>3</sub> emission profile, where short-

1 duration emission pulses vary in intensity by multiple orders of magnitude within a 4 h  
2 period. Further, the FG method provides an advantage over accumulating methods in that  
3 higher time resolution measurements subject to footprint distances that exceed the field  
4 boundary can be readily removed. It is therefore possible to collect more data when surface  
5 roughness and canopy height are low, corresponding to larger footprint distances. Such  
6 data are important to more fully understand the mechanism and profile of NH<sub>3</sub> fluxes.

7 Two different periods of elevated NH<sub>3</sub> emission were measured using the FG system:  
8 the first occurring during DOY 130 – 132, and the second during DOY 140 – 143. We  
9 attribute the timing and occurrence of these two distinct periods to environmental  
10 conditions (i.e., precipitation and soil temperature) and the use of urease inhibitor during  
11 fertilizer application. Previous studies have found elevated NH<sub>3</sub> emission to be correlated  
12 with higher temperatures (Sharpe and Harper, 1995; Balasubramanian et al., 2017). The  
13 highest FG<sub>30min</sub> emission (2312 ng m<sup>-2</sup> s<sup>-1</sup>) was observed in the afternoon on DOY 132. This  
14 was followed by intermittent precipitation beginning at 23:00 on DOY 132 through 12:30  
15 on DOY 136 resulting in a total rainfall during this period of 55 mm. Soil temperature  
16 subsequently reduced from 22.5 ± 2.8 °C on DOY 132 to a minimum of 11.6 ± 4.0 °C on DOY  
17 137 (where temperatures are reported as average of 26 daytime measurements), and  
18 lower NH<sub>3</sub> emission was observed. Soil temperature then increased, reaching 24.4 ± 4.9 °C  
19 on DOY 140, concurrent with the second elevated emission period.

20 Beside meteorological conditions, the timing of the NH<sub>3</sub> emission peaks can be  
21 influenced by the properties of the applied fertilizer. Walker et al. (2013), observed two  
22 periods of elevated NH<sub>3</sub> emission following application of 134 kg N ha<sup>-1</sup> UAN with



1 Agrotain®: one during the first week after fertilizer application ( $500 \text{ ng m}^{-2} \text{ s}^{-1}$ ) and a  
2 second during the third week after fertilizer application ( $700 \text{ ng m}^{-2} \text{ s}^{-1}$ ). Walker et al.  
3 (2013) attributed the emission profile to the effect of the urease inhibitor, where the first  
4 period is attributed to  $\text{NH}_4^+$  fraction of the UAN volatilizing as  $\text{NH}_3$ , and the second period  
5 corresponds to reduced effectiveness of the urease inhibitor, resulting in hydrolysis of urea  
6 to  $\text{NH}_4^+$  and subsequent volatilization as  $\text{NH}_3$ .

7 The profiles reported here and by Walker et al. (2013) differ from those reported by  
8 Rawluk et al. (2001) and Engel et al. (2011) during focused studies on the effect of urease  
9 inhibitor. In seven of eight field trials using chamber measurement methods, Rawluk et al.  
10 reported an emission profile with two periods of elevated  $\text{NH}_3$  emission in only one trial.  
11 Engel et al. (2011) reported  $\text{NH}_3$  emission peaks occurring 20 – 40 days after fertilizer  
12 application across 12 field trials, and presented no cases in which a bi-modal pattern of  
13 emission was observed. It is important to note that the study by Engel et al. was conducted  
14 over cold soils ( $-2$  to  $5 \text{ }^\circ\text{C}$ ), so the magnitude of the time delay is expected to be increased  
15 when compared with this study. However, both of these studies were conducted using  
16 integrated sampling methods, with averaging intervals of one to four days by Rawluk et al.,  
17 and five to seven days by Engel et al. Due to the short duration ( $< 2$  days) of the first  
18 elevated emission period reported both in results presented here and by Walker et al.  
19 (2013), it is possible that such a peak would not have been observed using longer  
20 averaging intervals (*i.e.*, days). Further research is required to quantify the effect of urease  
21 inhibitor at the field scale relative to local environmental conditions.

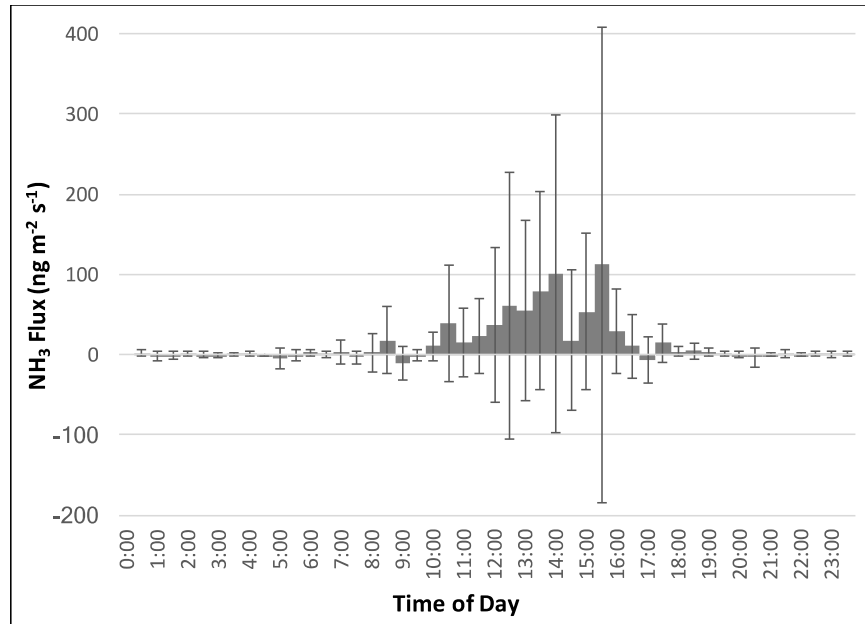
### 3.3 Diurnal $\text{NH}_3$ Emission

A dynamic deadband was used in the REA system to increase the relative measured concentration of  $\text{NH}_3$  in up- and down-draft denuders (Bowling et al., 1999). This approach helps to more effectively resolve  $\text{NH}_3$  flux during turbulent conditions but can result in reduced data quality during neutral and stable nighttime conditions. As such, the REA method as used in this field campaign is not a suitable approach to measure nighttime  $\text{NH}_3$  fluxes (Fotiadi et al., 2005).

Conversely, the FG method does not rely on turbulent eddies to trigger conditional sampling during up- and down-drafts. This enables the FG method to quantify flux across a broad range of atmospheric stability, including nighttime conditions. Additionally, the shorter 30 min averaging period reduces the impact of atmospheric non-stationarity on data quality. A clear diurnal pattern of  $\text{NH}_3$  flux was observed, in which the highest positive fluxes and greatest variability in flux (as characterized by standard deviation) occurred during daytime hours. Mean  $\text{NH}_3$  flux and standard deviation for each 30 min period across all qualified measurements are presented in Figure 5. We observe that there is a high variation in the measured fluxes. However, the measurements in general show upward fluxes, which are generally increasing in magnitude during the 09:00 – 16:00 period, while small upward or downward (depositional) fluxes are observed in the evening to early morning hours. This is consistent with the general understanding of bidirectional  $\text{NH}_3$  fluxes, controlled by aerodynamic ( $r_a$ ), quasi-laminar boundary layer ( $r_b$ ), and bulk surface resistances ( $r_c$ ), where  $r_a$  depends on meteorological and surface parameters (wind speed, air temperature, soil temperature, surface roughness length, leaf area index),  $r_b$  also

1 depends on meteorology and  $\text{NH}_3$  properties (i.e., solubility, reactivity) and molecular  
2 diffusivity and  $r_c$  on  $\text{NH}_3$  compensation points in soil and in canopy (Wesely, 1989, Nemitz  
3 et al., 2000). Presence of dew and thin water layers on leaves contribute to  $\text{NH}_3$  absorption  
4 and can account for the nighttime to early morning observed small upward or depositional  
5 fluxes (Nemitz et al., 2000). During daytime, increasing temperatures (affect dew  
6 evaporation, chemical equilibria at leaf, soil and stomatal resistance and the soil-air  
7 temperature differential), and changing atmospheric stability contribute to  $\text{NH}_3$  fluxes  
8 shifting upwards, and their magnitudes to increase. It is not possible to infer from the  
9 measurements the relative influence of  $r_a$ ,  $r_b$ ,  $r_c$ . A low average flux is observed between  
10 14:00 and 14:30 with an increased flux in the one hour period following that, with high  
11 variability. It is possible that a decrease in  $r_a$  and  $r_b$  due to a change in stability in mid-  
12 afternoon could result in higher dry deposition velocities (Liu et al., 2007).

13



1

2 **Figure 5:** Diurnal pattern of NH<sub>3</sub> flux as measured using the flux gradient method, where solid bars indicate  
 3 mean NH<sub>3</sub> flux during each 30 min period and error bars represent ± 1 standard deviation of the mean.

4 For the entire growing season, mean daytime FG<sub>30min</sub> flux was  $25.9 \pm 93.5 \text{ ng m}^{-2} \text{ s}^{-1}$ ,  
 5 while mean nighttime flux was  $-0.23 \pm 0.23 \text{ ng m}^{-2} \text{ s}^{-1}$ , where “daytime” is considered the  
 6 interval with net radiation value greater than 12 Watts m<sup>-2</sup> (EddyPro , Version 5.1.1, LI-  
 7 COR: Lincoln, NE). When calculated for the first 30 days after fertilizer application (DOY  
 8 126 – 156), mean daytime flux was  $53 \pm 159 \text{ ng m}^{-2} \text{ s}^{-1}$ , compared to nighttime flux of  $-0.5 \pm$   
 9  $9.0 \text{ ng m}^{-2} \text{ s}^{-1}$ . Following the first 30 days after fertilizer application, emission to the  
 10 atmosphere was markedly lower during the daytime for the subsequent 30-day period  
 11 (DOY 157 – 186), where daytime flux was  $1.4 \pm 21 \text{ ng m}^{-2} \text{ s}^{-1}$ , and  $0.04 \pm 2.1 \text{ ng m}^{-2} \text{ s}^{-1}$   
 12 during nighttime.

13 *3.4 Inter-Comparison of Concurrent Measurements*

14 After FG data qualification for  $r_{90\%} < 100 \text{ m}$  and  $r_{70\%} < 100 \text{ m}$ , remaining measurements  
 15 were compared to determine total concurrent samples (Table 2).

	Number of Measurements (N)		
	Total	r <sub>70%</sub> < 100 m	r <sub>90%</sub> < 100m
<b>REA</b>	39	23	22
<b>FG</b>	2782	1178	896
<b>Concurrent (4 h)</b>	10	10	7
<b>Concurrent (30 min)</b>	82	82	57

1 **Table 2:** Total number of relaxed eddy accumulation (REA) and flux gradient (FG) measurements, remaining  
2 qualified measurements after using 70% and 90% footprint distance, and concurrent REA and FG samples,  
3 where “4 h” indicates measurements were concurrent during the entire 4 h REA interval and “30 min”  
4 indicates a concurrent REA measurement occurred during a 30 min FG measurement.

5 The REA system was operated most regularly during the first 30 days after fertilizer  
6 application, as this was the period of greatest interest for NH<sub>3</sub> flux measurement (Nelson et  
7 al., 2017). Therefore, it was also expected that the most concurrent REA and FG  
8 measurements would occur during this part of the season. However, challenges associated  
9 with the operation of the FG system at the beginning of the season limited the total number  
10 of concurrent measurements during this period. For the 70% footprint condition, six  
11 concurrent measurements were collected between DOY 131-158, while three concurrent  
12 measurements were collected for the 90% footprint condition. Since the early-season  
13 period is of most interest for NH<sub>3</sub> emissions (Walker et al., 2013; Nelson et al., 2017), the  
14 70% footprint condition was used for the purpose of method inter-comparison discussed  
15 in this section (Table 3).

16

1

DOY	$\overline{F_{NH_3}}$ (ng m <sup>-2</sup> s <sup>-1</sup> )		
	REA (Nelson et al, 2017)	FG <sub>240min</sub> (r <sub>70%</sub> < 100 m)	FG <sub>240min</sub> (r <sub>90%</sub> < 100 m)
131	682.1	379.1	
132	799.6	752.6	
133	191.3	-35.9	
157	-8.5	5.0	5.0
158_1	130.8	-0.2	-0.2
158_2	254.5	-0.5	-0.5
178_1	-36.6	-0.1	-0.1
178_2	14.3	-0.1	-0.1
179_1	71.2	0.04	0.04
179_2	-44.8	0.01	0.01
<b>All</b>	<b>205 ± 300</b>	<b>110 ± 256</b>	<b>0.6 ± 2.0</b>

2 **Table 3:** Summary of all concurrent relaxed eddy accumulation (REA) and flux gradient (FG) measurements.  
3 REA measurements were footprint-corrected according to Nelson et al., 2017. FG measurements were  
4 averaged to a 4 h interval, after 70% and 90% footprint qualification, where \_1 and \_2 indicate morning and  
5 afternoon measurements, respectively.

6

7 *Correl(REA, FG)* for all concurrent r<sub>70%</sub> measurements, averaged to the 4 h REA  
8 averaging interval, was 0.91, indicating a strong correlation between the flux trends  
9 observed with both systems at the timescale of REA measurement. Measurements from  
10 both systems were in agreement using the Wilcoxon rank sum test at a 0.95 confidence  
11 level.

12 Later season REA flux measurements (*i.e.*, after DOY 157) were lower when compared  
13 with DOY 126-157, with mean measured flux of  $14 \pm 99.2$  ng m<sup>-2</sup> s<sup>-1</sup>. For concurrent  
14 samples during DOY 158-179, mean flux with REA was  $57.3 \pm 106$  ng m<sup>-2</sup> s<sup>-1</sup>, compared to -  
15  $0.50 \pm 5.10$  ng m<sup>-2</sup> s<sup>-1</sup> with FG<sub>240min</sub>. The FG method did not further resolve flux variability

1 with 30-min or 240-min measurements during this period ( $\overline{FG}_{30min} = 0.8 \pm 23.3 \text{ ng m}^{-2} \text{ s}^{-1}$ ;  
2  $\overline{FG}_{240min} = 1.1 \pm 7.1 \text{ ng m}^{-2} \text{ s}^{-1}$ ).

### 3 *3.5 Benefits and Limitations of Measurement Methods*

4 The REA method has been well-documented in literature for use in measuring trace  
5 atmospheric fluxes of  $\text{NH}_3$  from fertilized fields (Myles et al., 2007; Walker et al., 2013;  
6 Nelson et al., 2017). However, these field campaigns have either been focused on a short  
7 period (1 to 3 months) of the total growing season (Myles et al., 2007; Walker et al., 2013)  
8 or limited in total number of measurements ( $N = 35$ ) across a full growing season (Nelson  
9 et al., 2017). This is largely due to the labor required to operate an accumulating system  
10 coupled with the need for subsequent laboratory analysis of samples. It is necessary when  
11 operating such a system to have personnel on site at the beginning and end of each  
12 measurement interval. Further, samplers must be prepared and extracted in a controlled  
13 laboratory environment and stored under refrigeration. While not insurmountable, these  
14 challenges add to the complexity of using a REA system, under realistic field conditions.

15 The FG system was designed for near-autonomous, continuous operation under field  
16 conditions, though visits were required on a weekly basis to adjust the AEM and reference  
17 sonic anemometer and install a clean inlet. However, the complexity of the FG system led to  
18 additional downtime, due to equipment malfunctions and required frequent maintenance  
19 and adjustment. The length of the sampling line, combined with repeated vertical  
20 movement of the AEM resulted in kinking of the sampling line on multiple occasions.  
21 Challenges with the sampling line heater also resulted in condensation of water in the

1 sample lines during periods of high relative humidity. Future research focused on technical  
2 improvements of the system could resolve some of these issues.

3        Though the complete REA system does require more regular field visits for operation, it  
4 benefits from being relatively inexpensive (< \$10,000 equipment and installation costs) to  
5 deploy in the field. When compared with the complete FG system (> \$100,000 equipment  
6 and installation costs), the cost of deploying a REA system has significant advantages when  
7 seeking to measure NH<sub>3</sub> emissions from a diverse range of field conditions, crop types, and  
8 agricultural practices. However, for situations where it is desirable to obtain higher time  
9 resolution emission and deposition fluxes in the first several weeks after fertilizer  
10 application, the REA method cannot provide the high temporal resolution that is possible  
11 with FG.

#### 12 **4. Summary and Conclusions**

13        This research presents the first inter-comparison of NH<sub>3</sub> flux measurements using  
14 relaxed eddy accumulation (REA) and flux gradient (FG) systems in the USA. This inter-  
15 comparison was conducted above an intensively managed corn canopy in Central, Illinois,  
16 USA, thereby providing important new data regarding NH<sub>3</sub> fluxes under meteorological  
17 conditions in this area. Use of the FG system enabled temporal resolution of early-season  
18 peak fluxes greater than those previously reported using accumulating measurement  
19 methods. Results from the REA and FG system were highly correlated, with Pearson  
20 correlation of 0.91 between the two systems, when measurements at the same averaging  
21 time (4 h) were compared.



1 The FG system resolved two distinct periods of elevated early-season emission (DOY  
2 130 – 132 and DOY 140 – 143). This was made possible by the advantage of 30 min  
3 sampling and straightforward removal of data when large footprint conditions were  
4 observed. The ability to accurately quantify fluxes over the 4 h REA averaging interval was  
5 limited during the second elevated emission event due to high winds and low surface  
6 roughness. The two periods of elevated emissions are attributed to a combination of the  
7 effect of localized environmental conditions (*i.e.*, precipitation and soil temperature) and  
8 nBTPT urease inhibitor. Further research is needed to understand the extent of the impact  
9 of these factors on early-season emission and to improve evaluation of process-based  
10 models with increased temporal resolution (*i.e.*, < 1 h).

11 Inter-comparison of the two measurement methods indicated that both methods are in  
12 good agreement with respect to 4 h average NH<sub>3</sub> fluxes. The FG system was able to resolve  
13 temporal variability in 30-min intervals that was not possible using the REA system.  
14 However, it was also sensitive to mechanical failure and extreme weather conditions,  
15 which resulted in loss of data during the corn growth season. The REA method is labor-  
16 intensive and needs be supported by strict quality assurance and quality control  
17 procedures for measurement of the typically low ambient NH<sub>3</sub> concentrations. The  
18 integrated nature of REA sampling often necessitates long fetch that can be challenging to  
19 achieve in many field conditions. When taken with other measurement considerations such  
20 as cost of equipment and operation, it is clear that there are tradeoffs needing careful  
21 consideration before implementing the methods in different environments. In terms of the  
22 broader picture, the question remains open regarding how to upscale these local

1 measurements to the regional scale given the influences of environmental parameters,  
2 fertilizer properties, and method introduced variation. It appears that further method  
3 development and inter-comparison in diverse climatic, topographical, and land-use  
4 environments are essential to assist improved understanding of the spatial and temporal  
5 variability of biosphere-atmosphere NH<sub>3</sub> flux from agricultural fertilizer application and to  
6 facilitate evaluation of numerical emission and air quality models.

## 7 **5. Acknowledgements**

8 This study was funded by the National Science Foundation, Award Numbers AGS 12-  
9 36814 and AGS 12-33458, with an accompanying research experience for undergraduates  
10 (REU). The scientific results and conclusions, as well as any views or opinions expressed  
11 herein, are those of the author(s) and do not necessarily reflect the views of NSF, NOAA, or  
12 the Department of Commerce. The authors gratefully acknowledge the Energy Biosciences  
13 Institute and Mr. Timothy Mies and Mr. Collin Reeser for facilitating the use of the Energy  
14 Farm for the field campaign.

## 15 **References**

- 16 Appel, K. W., Foley, K. M., Bash, J. O., Pinder, R. W., Dennis, R. L., Allen, D. J., and Pickering, K.,  
17 2011. A multi-resolution assessment of the community multiscale air quality (CMAQ)  
18 model v4.7 wet deposition estimates for 2002–2006. *Geosci. Model Dev.* 4, 357-371.
- 19 Balasubramanian, S., Koloutsou-Vakakis, S., McFarland, D. M., and Rood, M. J., 2015.  
20 Reconsidering emissions of ammonia from chemical fertilizer usage in Midwest USA. *J.*  
21 *Geophys. Res. Atmos.* 120, 6232-6246.
- 22 Balasubramanian, S., Nelson, A., Koloutsou-Vakakis, S., Lin, J., Rood, M. J., Myles, LT. and  
23 Bernacchi C., 2017. Evaluation of DeNitrification DeComposition model for estimating  
24 ammonia fluxes from chemical fertilizer application. *Agr. Forest Meteorol.* 237-238, 123-  
25 134.

- 1 Baldocchi, D. D., Hincks, B. B., and Meyers, T. P. (1988). Measuring Biosphere-Atmosphere  
2 Exchanges of Biologically Related Gases with Micrometeorological Methods. *Ecology* 69,  
3 1331-1340.
- 4 Bash, J. O., Walker, J.T., Katul, G.G., Jones, M.R., Nemitz, E., and W. P. Robarge, 2010.  
5 Estimation of in-canopy ammonia sources and sinks in a fertilized zea mays field. *Environ.*  
6 *Sci. Technol.* 44, 1683-1689.
- 7 Bowling, D.R., Delany, A.C., Turnipseed, A.A., Baldocchi, D.D., Monson, R.K., 1999.  
8 Modification of the relaxed eddy accumulation technique to maximize measured scalar  
9 mixing ratio differences in updrafts and downdrafts. *J. Geophys. Res.* 104, 9121–9133.
- 10 Businger, J., and Oncley, S.P., 1990. Flux measurement and conditional sampling. *J. Atmos.*  
11 *Ocean Tech.* 7, 349-352.
- 12 Chadwick, D., Misselbrook, T., Gilhespy, S. Williams, J., Bhogal, A., Sagoo, L., Nicholson, F.,  
13 Webb, J., Anthony, S., Chambers, B., 2005. WP1b Ammonia emissions and crop N use  
14 efficiency. Component report for Defra Project NT2605 (CSA 6579).
- 15 Desjardins, R.L., 1972. A study of carbon-dioxide and sensible heat fluxes using the eddy  
16 correlation technique. *PhD dissertation* Cornell University, 189 pp.
- 17 Engel, R., Jones, C., Wallander, R., 2011. Ammonia Volatilization from Urea and Mitigation  
18 by NBPT following Surface Application to Cold Soils. *Soil Sci. Soc. Am. J.* 75, 2348–10.
- 19 Erisman, J. W., Galloway, J. N., Seitzinger, S., Bleeker, A., Dise, N. B., Petrescu, A. M., Leach, A.  
20 M., and de Vries, W., 2013. Consequences of human modification of the global nitrogen  
21 cycle. *Philos. T. R. Soc. B.* 368, 20130116.
- 22 Fenn, L.B., Hossner, L.R., 1985. Ammonia Volatilization from Ammonium or Ammonium-  
23 Forming Nitrogen Fertilizers, in: Stewart, B.A. (Ed.), *Advances in Soil Science*. Springer New  
24 York, pp. 123–169.
- 25 Ferrara, R.M., Loubet, B., Decuq, C., Palumbo, A.D., Di Tommasi, P., Magliulo, V., Masson, S.,  
26 Personne, E., Cellier, P., Rana, G., 2014. Ammonia volatilisation following urea fertilisation  
27 in an irrigated sorghum crop in Italy. *Agr. Forest Meteorol.* 195-196, 179–191.
- 28 Flechard, C.R., Massad, R.S., Loubet, B., Personne, E., Simpson, D., Bash, J.O., Cooter, E.J.,  
29 Nemitz, E., Sutton, M.A., 2013. Advances in understanding, models and parameterizations of  
30 biosphere-atmosphere ammonia exchange. *Biogeosciences* 10, 5183–5225.
- 31 Fotiadi, A. K., Lohou, F., Druilhet, A., Serça, D., Said, F., Laville, P., and Brut, A., 2005.  
32 Methodological development of the conditional sampling method. Part II: quality control  
33 criteria of relaxed eddy accumulation flux measurements. *Bound-Lay. Meteorol.* 117, 577-  
34 603.

- 1 Galloway, J. N., Townsend, A. R., Erisman, J. W., Bekunda, M., Cai, Z., Freney, J. R., Martinelli,  
2 L. A., Seitzinger, S. P., and Sutton, M. A., 2008. Transformation of the nitrogen cycle: recent  
3 trends, questions, and potential solutions. *Science* 320, 889-892.
- 4 Garcia, L., Générumont, S., Bedos, C., Simon, N.N., Garnier, P., Loubet, B., Cellier, P., 2012.  
5 Accounting for surface cattle slurry in ammonia volatilization models: the case of Volt'Air.  
6 *Soil Sci. Soc. Am. J.* 76, 2184-2194.
- 7 Gay, L. W., Fritschen, L. J., 1979. An exchange system for precise measurements of  
8 temperature and humidity gradients in the air near the ground. *Hydrology and Water*  
9 *Resources in Arizona and the Southwest*, 2986, 37-42.
- 10 Générumont, S., Cellier, P., 1997. A mechanistic model for estimating ammonia volatilization  
11 from slurry applied to bare soil. *Agr. Forest Meteorol.* 88, 145-167.
- 12 Green M. C., Chen L. W., DuBois D. W., and Molenaar J. V., 2012, Fine particulate matter and  
13 visibility in the Lake Tahoe Basin: chemical characterization, trends, and source  
14 apportionment. *J. Air Waste Manage.*, 62, 953-65.
- 15 Harper, L.A., Sharpe, R.R., 1995. Nitrogen Dynamics in Irrigated Corn: Soil-Plant Nitrogen  
16 and Atmospheric Ammonia Transport. *Agron. J.* 87, 669-675.
- 17 Hicks, B.B., and M.L. Wesely. 1978. An examination of some micrometeorological methods  
18 for measuring dry deposition. EPA Publ. EPA-600/7-78-116. USEPA, Research Triangle  
19 Park, NC.
- 20 Kljun, N., P. Calanca, M. W. Rotach, and H. P. Schmid., 2004. A simple parameterisation for  
21 flux footprint predictions. *Bound-Lay. Meteorol.* 112, 503-523.
- 22 Kormann R., Meixner F. X., 2001. An analytical footprint model for non-neutral  
23 stratification, *Bound-Lay. Meteorol.* 99, 207-224.
- 24 Li, Y., Schichtel, B.A., Walker, J.T., Schwede, D.B., Chen, X., Lehmann, C.M.B., Puchalski, M.A.,  
25 Gay, D.A., Collett, J.L., Jr., 2016. Increasing importance of deposition of reduced nitrogen in  
26 the United States. *Proc Natl Acad Sci USA* 113, 5874-5879.
- 27 Liu S., Lu L., Mao D., Jia L., 2007. Evaluating parameterizations of aerodynamic resistance to  
28 heat transfer using field measurements. *Hydrol. Earth Syst. Sci.*, 11, 769-783, [www.hydrol-](http://www.hydrol-)  
29
- 30 Loubet, B., Decuq, C., Personne, E., Massad, R.S., Flechard, C., Fanucci, O., Mascher, N.,  
31 Gueudet, J.C., Masson, S., Durand, B., Générumont, S., Fauvel, Y., Cellier, P., 2012. Investigating  
32 the stomatal, cuticular and soil ammonia fluxes over a growing tritical crop under high  
33 acidic loads. *Biogeosciences*, 9, 1537-1552.
- 34 Martin, N. A., Ferracci, V., Cassidy, N., and Hoffnagle, J. A., 2016. The application of a cavity  
35 ring-down spectrometer to measurements of ambient ammonia using traceable primary  
36 standard gas mixtures. *Applied Physics B*, 122(8), 219, doi:10.1007/s00340-016-6486-9.

- 1 McCarthy, J. 1973. A method for correcting airborne temperature data for sensor response  
2 time. *J. Appl. Meteorol.* 12: 211–214.
- 3 Meyers, T. P., Hall, M. E., Lindberg, S. E., Kim, K., 1996. Use of the modified Bowen-ratio  
4 technique to measure fluxes of trace gases. *Atmos. Environ.*, 30, 3321 – 3329.
- 5 Meyers, T., Luke, W., Meisinger, J., 2006. Fluxes of ammonia and sulfate over maize using  
6 relaxed eddy accumulation. *Agr. Forest Meteorol.* 136, 203–213.
- 7 Milford, C., Theobald, M. R., Nemitz, E., Hargreaves, K. J., Horvath, L., Raso, J., Dämmgen, U.,  
8 Neftel, A., Jones, S. K., Hensen, A., Loubet, B., Cellier, P., and Sutton, M. A., 2009. Ammonia  
9 fluxes in relation to cutting and fertilization of an intensively managed grassland derived  
10
- 11 Miller, D.J., Sun, K., Tao, L., Khan, M.A., Zondlo, M.A., 2014. Open-path, quantum cascade-  
12 laser-based sensor for high-resolution atmospheric ammonia measurements. *Atmos. Meas.*  
13 *Tech.* 7, 81–93.
- 14 Moosmüller, H., Varma, R., Arnott, W. P., 2005. Cavity ring-down and cavity-enhanced  
15 detection techniques for the measurement of aerosol extinction. *Aerosol Science and*  
16 *Technology*, 39, 30-39.
- 17 Myhre, G., Shindell, D., Bréon, F.M., Collins, W., Fuglestedt, J., Huang, J., Koch, D., Lamarque,  
18 J.-F., Lee, D., Mendoza, B., Nakajima, T., Robock, A., Stephens, G., Takemura, T. and Zhang, H.,  
19 2013. Anthropogenic and natural radiative forcing. In: *Climate Change 2013: The Physical*  
20 *Science Basis. Contribution of Working Group I to the Fifth Assessment Report of the*  
21 *Intergovernmental Panel on Climate Change [Stocker, T.F., D. Qin, G.-K. Plattner, M. Tignor,*  
22 *S.K. Allen, J. Boschung, A. Nauels, Y. Xia, V. Bex and P.M. Midgley (eds.)]. Cambridge*  
23 *University Press, Cambridge, United Kingdom and New York, NY, USA.*
- 24 Myles, L., Meyers, T.P., Robinson, L., 2007. Relaxed eddy accumulation measurements of  
25 ammonia, nitric acid, sulfur dioxide and particulate sulfate dry deposition near Tampa, FL,  
26 USA. *Environ. Res. Lett.* 2, 034004.
- 27 Myles, L., Kochendorfer, J., Heuer, M. W., and Meyers, T. P., 2011. Measurement of trace gas  
28 fluxes over an unfertilized agricultural field using the flux-gradient technique. *J. Environ.*  
29 *Qual.* 40, 1359-65.
- 30 NADP (2012) Standard Operating Procedure for Preparation and Extraction of URG  
31 Denuders. SOP Number PR-4074, Revision 1.1.
- 32 Nelson, A.J., Koloutsou-Vakakis, S., Rood, M.J., Myles, L., Lehmann, C., Balasubramanian, S.,  
33 Joo, E. Heuer, M., Vieira-Filho, M., Lin, J. 2017. Season-long ammonia flux measurements  
34 above fertilized corn in central Illinois, USA, using relaxed eddy accumulation. *Agr. Forest*  
35 *Meteorol.*, 239, 202-212.
- 36 Nelson, A. J; Lichiheb, N.; Koloutsou-Vakakis, S.; Rood, M. J.; Heuer, M.; Myles, L.; Joo, E.;  
37 Miller, J.; Bernacchi, C. 2018. Data for Ammonia Flux Measurements above a Corn Canopy

- 1 using Relaxed Eddy Accumulation and a Flux Gradient System. University of Illinois at  
2 Urbana-Champaign. [https://doi.org/10.13012/B2IDB-0071156\\_V1](https://doi.org/10.13012/B2IDB-0071156_V1).
- 3 Nemitz, E., M. A. Sutton, J. K. Schjoerring, S. Husted, and G. P. Wyers, 2000, Resistance  
4 modelling of ammonia exchange above oilseed rape, *Agric. Forest Meteorol.*, 105(4), 405–  
5 425.
- 6 Personne, E., Loubet, B., Herrmann, B., Mattsson, M., Schjoerring, J.K., Nemitz, E., Sutton,  
7 M.A., Cellier, P. 2009. SURFATM-NH<sub>3</sub>: a model combining the surface energy balance and  
8 bi-directional exchanges of ammonia applied at the field scale. *Biogeosciences*, 6:1371–  
9 1388.
- 10 Personne, E., Tardy, F., Générumont, S., Decuq, C., Gueudet, J.-C., Mascher, N., Durand, B.,  
11 Masson, S., Lauransot, M., Fléchar, C., Burkhardt, J., Loubet, B., 2015. Investigating sources  
12 and sinks for ammonia exchanges between the atmosphere and a wheat canopy following  
13 slurry application with trailing hose. *Agric. For. Meteorol.*, 207, 11-23.
- 14 Pinder, R.W., Adams, P.J., Pandis, S.N., 2007. Ammonia Emission Controls as a Cost-Effective  
15 Strategy for Reducing Atmospheric Particulate Matter in the Eastern United States.  
16 *Environ. Sci. Technol.* 41, 380–386.
- 17 Rawluk, C.D.L., Grant, C.A., Racz, G.J., 2001. Ammonia volatilization from soils fertilized with  
18 urea and varying rates of urease inhibitor NBPT. *Can. J. Soil. Sci.* 81, 239–246.
- 19 Scherer, J. J., Paul, J.B., O’Keefe, A., Saykally, R.J., 1997. Cavity ringdown laser absorption  
20 spectroscopy: History, development, and application to pulsed molecular beams. *Chem.*  
21 *Rev.* 97, 25-51.
- 22 Sharpe, R.R., Harper, L.A., 1995. Soil, plant and atmospheric conditions as they relate to  
23 ammonia volatilization. *Fertil. Res.* 42, 149–158.
- 24 Sintermann, J., Spirig, C., Jordan, A., Kuhn, U., Ammann, C., Neftel, A., 2011. Eddy covariance  
25 flux measurements of ammonia by high temperature chemical ionisation mass  
26 spectrometry. *Atmos. Meas. Tech.*, 4, 599-616.
- 27 Spindler, G., Teichmann, U. and Sutton, M.A., 2001. Ammonia dry deposition over grassland-  
28 micrometeorological flux-gradient measurements and bidirectional flux calculations using  
29 an inferential model. *Quarterly Journal of the Royal Meteorological Society*, 127, 795-814.
- 30 Sun, K. Tao, L., Miller, D.J., Zondlo, M.A., Shonkwiler, K.B., Nash, C., Ham, J.M., 2015. Open-  
31 path eddy covariance measurements of ammonia fluxes from a beef cattle feedlot. *Agr.*  
32 *Forest Meteorol.* 213, 193–202.
- 33 Sutton, M. A., Milford, C., Nemitz, E., Theobald, M. R., Hill, P. W., Fowler, D., Schjoerring, J. K.,  
34 Mattsson, M. E., Nielsen, K. H., Husted, S., Erisman, J. W., Otjes, R., Hensen, A., Mosquera, J.,  
35 Cellier, P., Loubet, B., David, M., Générumont, S., Neftel, A., Blatter, A., Herrmann, B., Jones, S.  
36 K., Horvath, L., Föhner, E., Mantzanas, K., Koukoura, Z., Gallagher, M., Williams, P., Flynn, M.,

1 and Riedo, M., 2011. Biosphere-atmosphere interactions of ammonia with grasslands:  
2 experimental strategy and results from a new European initiative, *Plant Soil*, 228, 131–145.

3 Sutton, M. A., Nemitz, E., Erisman, J. W., Beier, C., Bahl, K. B., Cellier, P., de Vries, W., Cotrufo,  
4 F., Skiba, U., Di Marco, C., Jones, S., Laville, P., Soussana, J. F., Loubet, B., Twigg, M., Famulari,  
5 D., Whitehead, J., Gallagher, M. W., Neftel, A., Flechard, C. R., Herrmann, B., Calanca, P. L.,  
6 Schjoerring, J. K., Daemmgen, U., Horvath, L., Tang, Y. S., Emmett, B. A., Tietema, A.,  
7 Penuelas, J., Kesik, M., Brueggemann, N., Pilegaard, K., Vesala, T., Campbell, C. L., Olesen, J. E.,  
8 Dragosits, U., Theobald, M. R., Levy, P., Mobbs, D. C., Milne, R., Viovy, N., Vuichard, N., Smith,  
9 J. U., Smith, P., Bergamaschi, P., Fowler, D., and Reis, S., 2007. Challenges in quantifying  
10 biosphere-atmosphere exchange of nitrogen species. *Environ. Pollut.* 150, 125-39.

11 UI, 2009. Illinois Agronomy Handbook, 24<sup>th</sup> edition. University of Illinois Extension.

12 USDA (2015), Illinois Corn County Estimates, Available from:  
13 [https://www.nass.usda.gov/Statistics\\_by\\_State/Illinois/Publications/County\\_Estimates/2](https://www.nass.usda.gov/Statistics_by_State/Illinois/Publications/County_Estimates/2014/IL_Corn_Production_by_County.pdf)  
14 [014/IL\\_Corn\\_Production\\_by\\_County.pdf](https://www.nass.usda.gov/Statistics_by_State/Illinois/Publications/County_Estimates/2014/IL_Corn_Production_by_County.pdf). Last Accessed September 2017.

15 USEPA (2011), Reactive Nitrogen in the United States: An Analysis of Inputs, Flows,  
16 Consequences, and Management Options. Available from: <http://www.epa.gov/sab>. Last  
17 accessed August 2017.

18 USEPA (2017), The 2011 National Emissions Inventory, Available from:  
19 <http://www.epa.gov/ttnchie1/net/2011inventory.html>. Last accessed September 2017.

20 Walker, J.T., Jones, M.R., Bash, J.O., Myles, L., Meyers, T., Schwede, D., Herrick, J., Nemitz, E.,  
21 Robarge, W., 2013. Processes of ammonia air–surface exchange in a fertilized *Zea mays*  
22 canopy. *Biogeosciences* 10, 981–998.

23 Watson, C.J., Miller, H., Poland, P., Kilpatrick, D.J., Allen, M.D.B., Garrett, M.K., Christianson,  
24 C.B., 1994. Soil Properties and the Ability of the Urease Inhibitor N-(n-BUTYL)  
25 Thoiphosphoric Triamide (nBTPT) to Reduce Ammonia Volatilization from Surface-Applied  
26 Urea. *Soil Biology and Biochemistry* 26, 1165–1171.

27 Wesely, M. L., 1989. Parameterization of surface resistances to gaseous dry deposition in  
28 regional-scale numerical models, *Atmos. Environ.*, 23, 1293–1304.

29 Vaittinen, O., Metsälä, M., Persijn, S., Vainio, M. and Halonen, L., 2014. Adsorption of  
30 ammonia on treated stainless steel and polymer surfaces. *App. Phys. B*, 115, 185-196.

31 Bobruzki, von, K., Braban, C.F., Famulari, D., Jones, S.K., Blackall, T., Smith, T.E.L., Blom, M.,  
32 Coe, H., Gallagher, M., Ghalaieny, M., McGillen, M.R., Percival, C.J., Whitehead, J.D., Ellis, R.,  
33 Murphy, J., Mohacsi, A., Pogany, A., Junninen, H., Rantanen, S., Sutton, M.A., Nemitz, E., 2010.  
34 Field inter-comparison of eleven atmospheric ammonia measurement techniques. *Atmos.*  
35 *Meas. Tech.* 3, 91–112.

36 Zhu, T., Pattey, E., Desjardins, R.L., 2000. Relaxed Eddy-Accumulation Technique for  
37 Measuring Ammonia Volatilization. *Environ. Sci. Technol.* 34, 199–203.